UCBNE-5102

REPROCESSABILITY AND PERFORMANCE IN GEOLOGIC REPOSITORY OF MONO-NITRIDE FUEL

Contribution to LDRD Project, Titled "Mono-Nitride Fuel Development for STAR and Space Applications"

Joonhong Ahn

Department of Nuclear Engineering
University of California, Berkeley

September 2005

The authors invite comments and would appreciate
being notified of any errors in the report.

Joonhong Ahn
Department of Nuclear Engineering
University of California
Berkeley, CA 94720
USA

ahn@nuc.berkeley.edu

Table of Contents

List of Tables

Table of Figures

I. Scope of Work

I.A. Objective:

This LDRD project is aimed at establishing fundamental bases for manufacturing and modeling capabilities for mono-nitride fuel. In the modeling capability area, the team at UCB will be in charge of analyzing (1) reprocessing processes for nitride fuels and (2) performance and safety of nitride fuel if it is disposed of in a geologic repository, such as Yucca Mountain repository.

I.B. Background:

The three-year LDRD is being carried out at Lawrence Livermore National Laboratory, to initiate advanced fuel development effort at LLNL and enhance its capability in material sciences research and manufacturing for mono-nitride fuel for the use in compact long-life reactors such as a liquid-metal cooled small reactor (SSTAR) and a light liquid-cooled reactor designed for space applications.

In the first and second years, various computer codes were acquired and modified for fuel performance and burn-up of nitride fuel. A lab-scale uranium-based nitride fuel manufacturing system was installed at LLNL. A flow sheet for nitride fuel fabrication was developed. With the system, a few sintered pellets of UN were made. UN and UN+ZrN+HfN were compared from various viewpoints including compactness, proliferation resistance, and fuel safety.

The tasks to be performed by the team at UCB will add important viewpoints for comparison, i.e., reprocessability and repository performance.

I.C. Scope of Work:

The following areas of work are to be addressed by the UCB team:

Task 1: Preliminary literature survey for (1) reprocessing of irradiated mono-nitride fuel and for (2) geochemical reactions of nitride fuel with groundwater

Task 2: Analyses on reprocessing process for mono-nitride fuel

Task 3: Analyses on dissolution mechanisms of nitride fuel in geologic environment to evaluate performance in a geologic repository.

Task 4: Prepare input for the LDRD final report. The UCB study report will be combined with the reports on other activities in the project.

II. Executive Summary

To investigate reprocessability and performance in a geologic repository for mono-nitride fuel, mathematical models have been developed.

For reprocessability, a pyrochemical process method is considered because evolution and recycle of N-15 gas can be handled. A simplified model reprocessing scheme has been analyzed for the separation of uranium mono-nitride fuel from cerium mono-nitride with a multi-stage extraction system. The distribution coefficient obtained from an optimized single-stage extraction system has been utilized as input data for a multi-stage extraction system. With 10 stages, the overall purity of the recovered uranium was 98.9% in the multi-stage extraction system with a net uranium recovery of 79%.

For repository performance, the dissolution rate for UN would be much lower than that for U metal but higher than that of uranium silicide. The reported high dissolution rates of UN in water at ~ 92°C indicate that UN is not stable in the hot aqueous environment. The numerical evaluation, based on the assumption that the dissolution rate of UN spent fuel is 10 times greater than those for UO_2 and borosilicate glass, indicates that the dissolution of UN spent fuel would complete within the time duration comparable to the half-life of Pu-239.

Thus, while UN may be a good fuel for a reactor that uses a non-aqueous coolant and is operated with a reprocessing option, spent UN fuel will be poor waste form for permanent disposal in a geologic repository because of its reactivity in an aqueous environment.

III. Reprocessability Analysis

III.A. Introduction

Uranium mononitride is being considered as a potential nuclear fuel for encapsulated nuclear heat sources, transmutation of toxic long-lived actinides, and space satellite missions. Numerous reactor performance studies have been performed with UN and it has been determined that the fuel has several desirable properties, which triggered an increased interest in the fuel.

Uranium mononitride is oxidized by heated water vapor, generating ammonia[1]:

$2UN + 4H_2O \rightarrow 2UO_2 + 2\,NH_3 + H_2$

Thus, with an appropriate pre-treatment, UN spent fuel can be reprocessed by conventional PUREX process. However, mainly because of a potential problem of evolution and recycle of nitrogen-15 gas[2], pyrochemical processes have been considered suitable, and studied actively for this type of fuel.

The present work will focus on a pyrochemical processing method. The system is shown in **Figure III.1**.

III.B. Single-Stage Molten-Salt/Liquid Metal Extraction System.

Figure III.2 below shows a schematic of a single-stage molten-salt/liquid metal extraction system. In the diagram, it is assumed that initially no uranium or cerium are present in the molten-salt phase. Additionally, bismuth and potassium are non-interacting spectator metals in the system. Initially the liquid metal phase containing the lithium reductant is contacted with the molten-salt phase. After a four-hour equilibrium, the phases are cooled and separated. The reductant is molten lithium; the actinides act as the corresponding oxidants. The following equations describe the interactions in the system:

UCl_3 (salt) + 3Li (metal) $\leftrightarrow$ U (metal) + 3LiCl (salt) $\quad K_U = 1.12 \times 1012 \quad$ [1]

$CeCl_3$ (salt) + 3Li (metal) $\leftrightarrow$ Ce (metal) + 3LiCl (salt) $\quad K_{Ce} = 5.75 \times 108 \quad$ [2]

Notice that the equilibrium constant for the uranium reduction is several orders of magnitude higher than the corresponding cerium reduction. This leads us to conclude that

---

[1] Bridger et al., Oxidation and hydrolysis of uranium and plutonium nitrides, *Reactivity in Solids, Proceedings of an International Symposium,* Wiley-Interscience, New York, NY, 389-400, 1969.

for any system, more uranium will always be recovered than cerium except in the limiting case that the mass of UCl_3 is infinitesimal relative the cerium chloride. Note also that given the high equilibrium constants, it is also possible for $CeCl_3$ to *reduce* UCl_3:

UCl_3 (salt) + Ce (metal) $\leftrightarrow$ $CeCl_3$ (salt) + U (metal) $\quad K_U' = 1.95 \times 10^3$ **[3]**

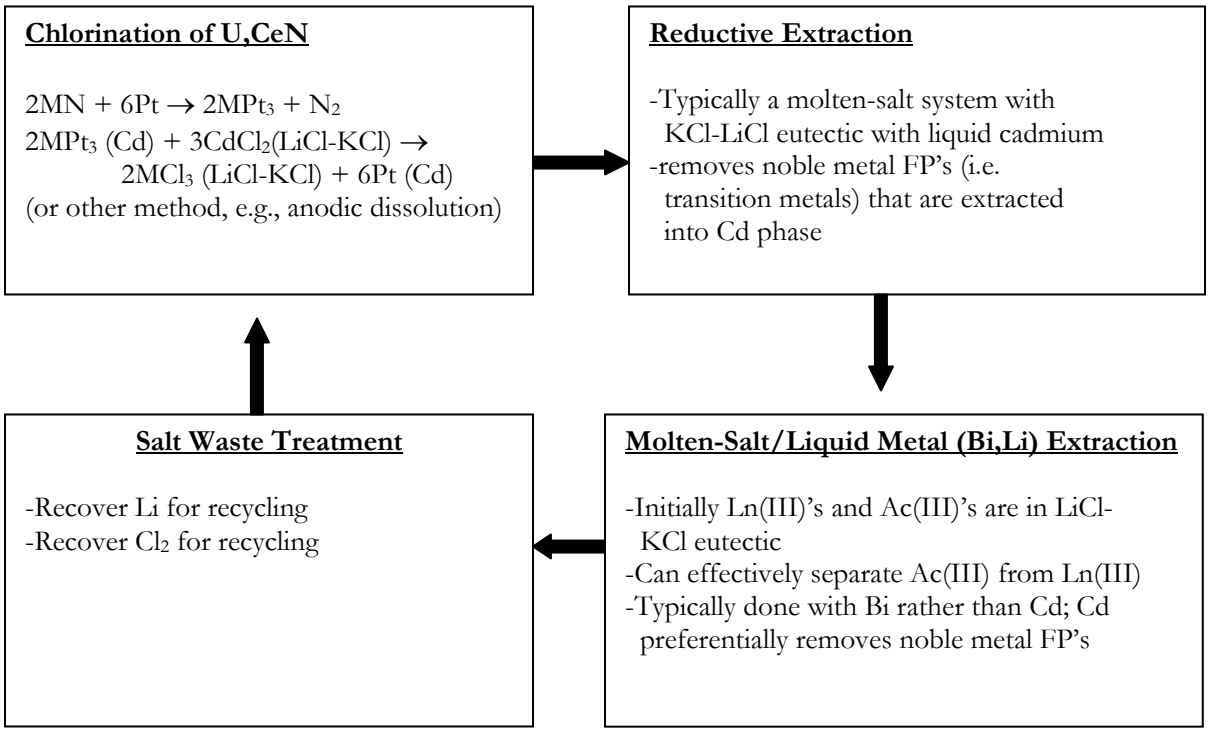

Figure III.1: A pyrochemical treatment of uranium mononitride[3].

The magnitude of equilibrium constant for equation **[3]** implies that the extent of reduction of uranium due to cerium metal is essentially negligible. Thus, in this work, the reduction due to cerium will be neglected.

Several Mass Balance Equations must be introduced so that distribution coefficients for each reacting component of the system can be calculated. **Figure III.3** is a collection of all the mass balance equations considered for the calculations. Here μ_j^0 refers to the initial mass of the jth species in the **salt** phase (e.g., Ce, U) and m_j^0 refers to the jth species in the metal phase initially. Non-superscripted values correspond to the *equilibrium* mass of the species. The values used for this work are shown below in **Table III.1**.

---

[2] T. Mukaiyama, OMEGA Program in Japan and ADS Development at JAERI, *Proc. 3rd Int. Conf. Accelerator Driven Transmutation Technologies and Applications,* Prague , 7 - 11 June 1999, Czech Republic.
[3] Kinoshita, et. al. *J. Nuc. Sci. Tech.*, **36**, 2, 189-197.

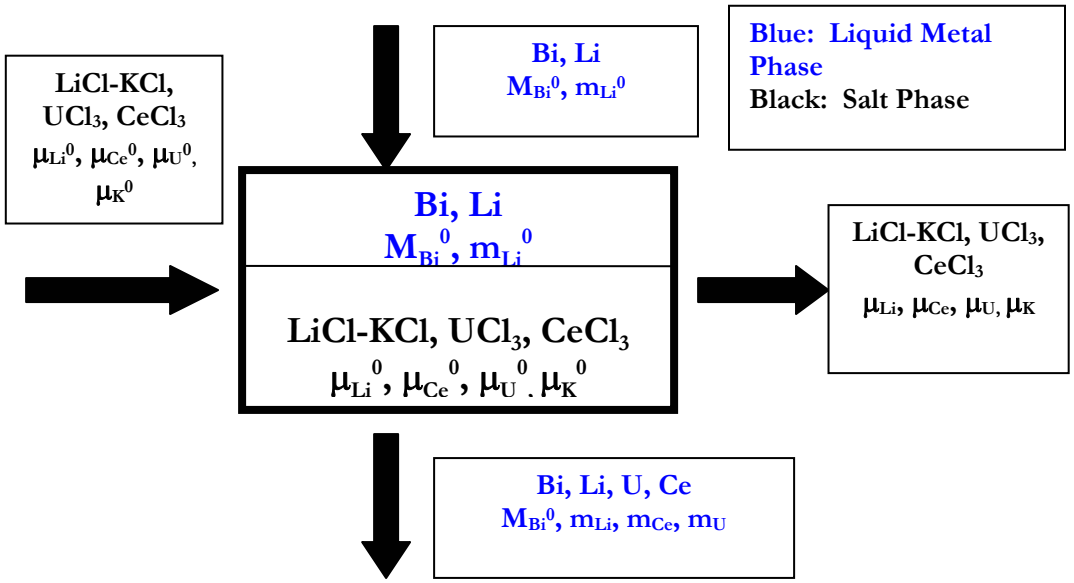

Figure III.2: Simple Molten-Salt/Liquid Metal Extraction System. Here Li is the reductant and the actinide chloride is the oxidant.

$\mu_{TOT} = \mu_{Li} + \mu_K^0 + \mu_U + \mu_{Ce}$ Salt Phase Mass Balance
$m_{TOT} = m_{Bi}^0 + m_{Li} + m_U + m_{Ce}$ Liquid Metal Phase Mass Balance
$\mu_U^0 = \mu_U + m_u$ Total Uranium Balance
$\mu_{Ce}^0 = \mu_{Ce} + m_{Ce}$ Total Cerium Balance
$\mu_{Li}^0 + m_{Li}^0 = \mu_{Li,i} + m_{Li}$ Total Lithium Balance
$m_{Li,i}^0 - m_{Li,i} = 3m_{Ce,i} + 3m_U$ An "Electron Balance"
$D_{j,I} = X_{j,i}/Y_{j,j} = (\mu_{j,i}/m_{j,i}*r)$ Distribution Coefficient.

Figure III.3: Mass Balance Equations Utilized for Optimization of the Single-Stage Extraction System.

Table III.1: Initial Input conditions for the single stage extraction system.

1) **Parameter**	1) **Value**
2) μ_K^0	2) 0.65 mol
3) μ_{Li}^0	3) 0.95 mol
4) μ_U^0	4) 2.5×10^{-4} mol
5) μ_{Ce}^0	5) 2.5×10^{-3} mol
6) M_{Bi}^0	6) 0.25 mol
7) m_{Li}^0	7) 0.00123 mol
8) K_U	8) 1.12×10^{12}
9) K_{Ce}	9) 5.75×10^8
10) R	10) 0.150
11) $q_{Ce} = q_U$	11) 3

III.C. Results

Figure III.4 shows the extracted uranium as a function of initial lithium loading. As expected, increasing the initial lithium loading increases the amount of extracted uranium increases. With this fact in mind, it would seem that higher quantities of lithium are required to extract the most uranium. However, although the preference of lithium to reduce UCl_3 is greater than that of $CeCl_3$, $CeCl_3$ is also reduced in some quantity. As

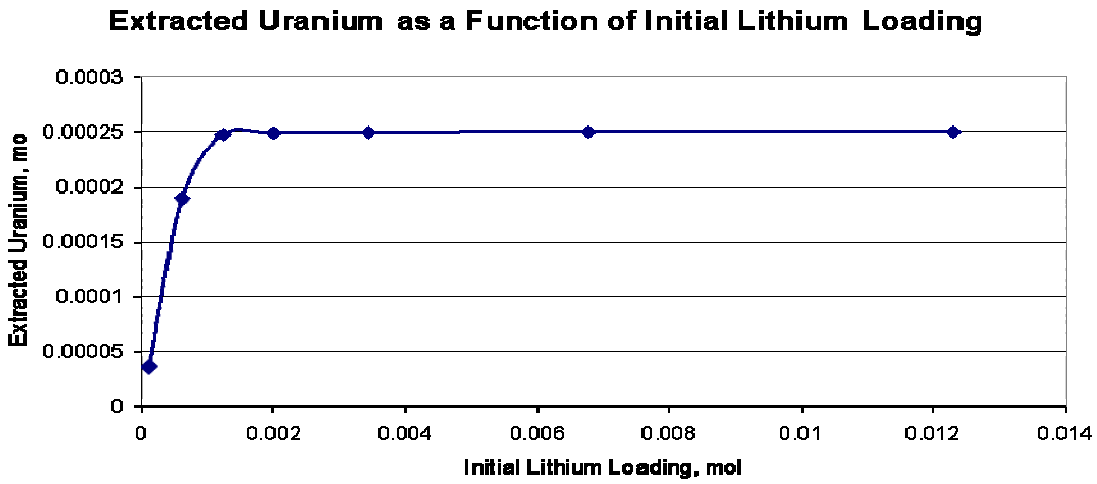

Figure III.4: Extracted Uranium as a Function of Initial Lithium loading.

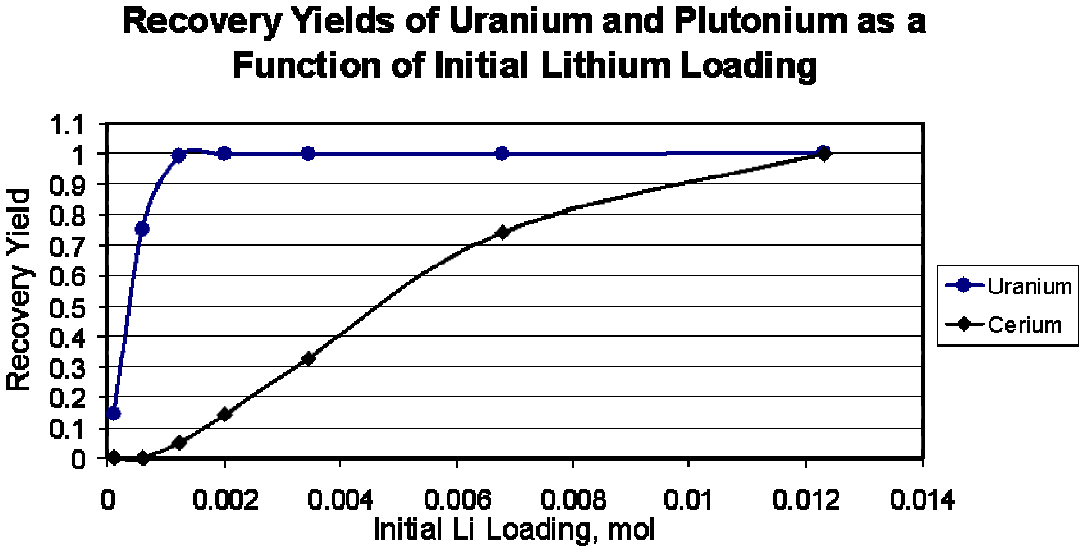

Figure III.5: Recovery Yields of Uranium and Plutonium as a Function of Initial Li loading.

Table III.1 showed, in this system there is more CeCl3 than UCl3 by an order of magnitude. Thus, although more uranium is recovered, there is similarly more cerium recovered. Figure III.5 illustrates this.

Finally, the recovery yield of the uranium tended to decrease with increasing purity. This is depicted in **Figure III.6** below. Because the purity of an extracted metal is typically a more important concern than recovery yield, the system values were optimized at a low initial lithium loading (0.000123 mol). To increase the overall yield of uranium with a similar purity, a multi-stage extraction system was developed. It was hoped that several extractions with small recovery yields would give an overall higher recovery yield after n stages than a single-stage extraction system.

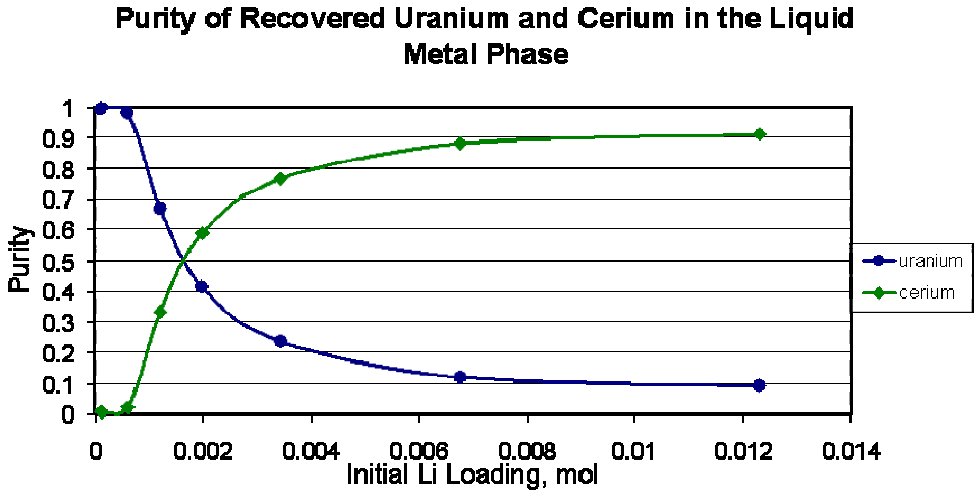

Figure III.6: Purity of U and Ce as a Function of Initial Lithium Loading

III.D. Multi-Stage Extraction System

Figure III.7 below shows a typical extraction system used for this work.

In this system, a liquid metal phase is contacted with a salt phase. After an equilibrium time, the two phases are decreased and the liquid metal phase collected. The process is repeated whereby the liquid phase is removed and replaced with a fresh quantity of liquid metal. Computationally, the only difference in this system from the single-stage extraction is that the equilibrium concentration for the first stage is equivalent to the initial input value for the next stage. The mass balance equations are the same as those listed in **Figure II.2** above.

The distribution coefficient that corresponded to the highest purity and lowest recovery yield was utilized to maintain the purity of the recovered uranium in each step. Using this

value, it could be determined the initial lithium loading mass m_{Li}^0 at each stage.

Figure III.8 shows the cumulative recovery yield and purity calculated in this work. Although the purity slightly decreased at each step, there was a cumulative purity of 98.9%. More work must be done to determine why the purity decreased at each step.

In theory, one can determine the number of stages required to extract all of the uranium from the liquid phase by extrapolating the cumulative recovery yield to 1. The cumulative uranium purity at that stage would give an idea of the overall purity of the uranium at nearly 100% separation.

Also, if both curves are extrapolated to the point where they cross, one can determine the number of stages that optimizes both the yield and the purity (both near 100%).

As a proof of concept measurement the values were obtained for a ten-stage system since most literature quotes five to ten stages. After 10 stages, the cumulative purity was determined to by 98.9%; the cumulative yield was only 79%.

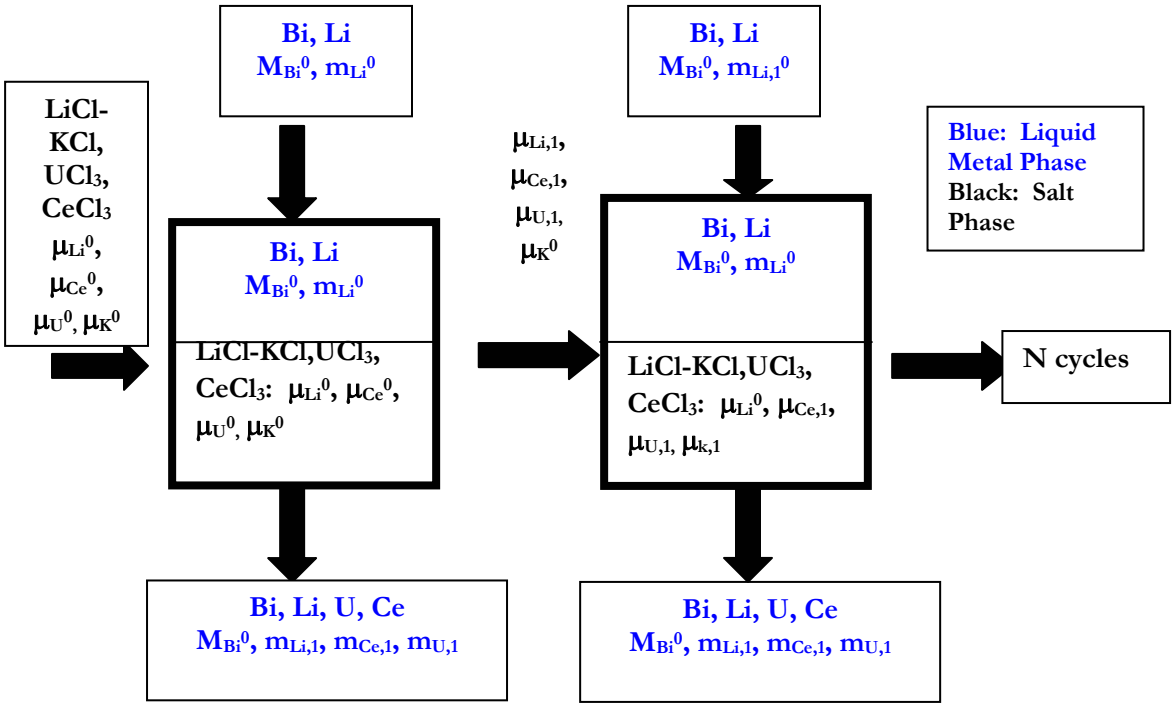

Figure III.7: Multi-Stage Extraction System.

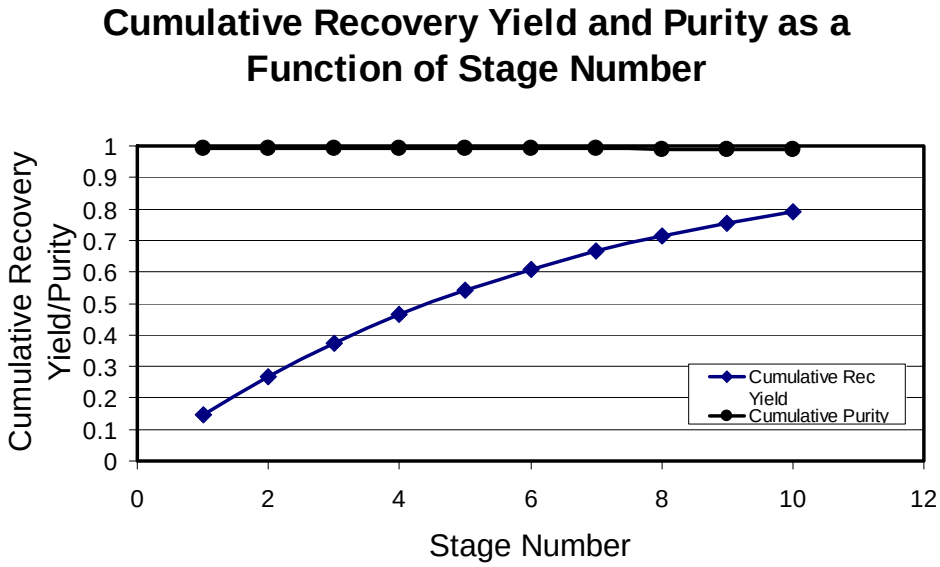

Figure III.8: Cumulative Purity and Recovery Yield as a function of stage number. Note the steady increase in recovery but slight decrease in purity.

III.E. Summary

In general, the net recovery yield of uranium from the multi-stage extraction was higher after 10 stages than in the simple single-stage extraction step. However, the net purity of the uranium extracted seemed to decrease slightly after each extraction, leading to a net purity of 98.9% as opposed to 99.4% extraction in the single-stage extraction system. This fact appears to be a result of one of two things. First, the constant lithium distribution coefficient may be invalid in that it slightly overestimates the amount of lithium loading needed for each step. This overestimate causes more cerium to be extracted as well. At each step there needs to be a new iteration to find the lithium distribution coefficient with an initial mass loading guess.

The value of r, 0.150, was assumed to be constant. This is perhaps a poor approximation because after each extraction, the liquid metal phase is removed and replaced by fresh Bi-Li alloy. Also, if the amounts of bismuth and potassium are supposedly constant, it would be necessary to recalculate r because the mass ratios are no longer constant. Because such an assumption was made for this project, the value "r" would need to be recalculated for each stage. Otherwise, the total amount of mass in each phase may be made to be constant by varying the initial potassium and bismuth masses but that would change the composition of each phase. For an accurate model of the system, such changes have to

be taken into account. Either of the abovementioned situations may explain the slight decrease in purity values.

In the future, this system may be compared to a "counter-current" multi-stage extraction system. The major difference between this system and the multi-stage extraction system proposed in this work is that instead of removing each liquid metal phase after equilibration, it is shuffled into a second stage with a counter-flowing salt phase that contacts the liquid metal phase and is equilibrated. It is expected that this system will generate higher recoveries and purities over fewer stage numbers because in each stage of the extraction, the liquid metal stage is in contact with fresh salt phase. The net effect is that the purity and recovery yield of the uranium in the metal phase increases steadily because the liquid metal phase is essentially "scrubbed" by the salt phase.

IV. Repository Performance Analysis

IV.A. Introduction

To consider repository performance for high-level waste (HLW), the principal importance is the rate of dissolution of matrix material by reacting with groundwater in repository environment. The rate of dissolution into groundwater is determined by various factors, such as in-package chemistry and temperature, which are determined by drift tunnel layout in the repository, hydro-geological conditions in the host rock, chemical compositions of groundwater, and materials contained in the waste package.

The matrix material is either fuel material itself in case spent fuel is directly disposed of, or solidification material after reprocessing such as borosilicate glass. The matrix is the principal material in the waste package, and determines in-package chemistry.

In the present analysis, we consider the case for direct disposal of UN spent fuel in Yucca Mountain Repository (YMR). For the case of disposal of solidified HLW resulting from reprocessing of spent UN fuel, previous results for defense HLW (DHLW) vitrified by borosilicate glass are used by assuming dissolution of borosilicate glass is the same for both cases.

For scoping evaluations attempted in this study, a model has been established for dissolution of the matrix material and cumulative release of radionuclides from the matrix to the surrounding environment. While numerical results are shown for matrix dissolution only, radionuclide release can also be evaluated numerically with the model once radionuclide compositions in the matrix are given.

IV.B. Model

In this study, radionuclides are considered to exist in the environment after released from a failed waste package, and to become environmental impact of the repository. In reality, some radionuclides released from failed packages still exist within engineered barriers such as the drip shield or in the near-field host rock included in the repository region, which could be excluded from repository impact consideration. With this simplification, the mass $W_i(t)$ of radionuclide i in the environment can be conservatively overestimated.

For the time period between the time of emplacement of the waste packages in the repository ($t = 0$) and the time of waste package failure ($t = T_f$), no radionuclides are

assumed to be released into the environment, but within waste packages the radionuclide composition changes with time due to radioactive decay. Therefore, for the mass $W_i(t)$ of radionuclide *i* in the environment,

$$W_i(t) = 0,\ 0 \le t \le T_f,\ i = 1, 2, \ldots. \quad (1)$$

For the mass in a single waste package $M_i(t)$, the governing equation is written as

$$\frac{dM_i(t)}{dt} = -\lambda_i M_i(t) + \lambda_{i-1} M_{i-1}(t),\ 0 < t \le T_f,\ i = 1, 2, \ldots,\ \lambda_0 \equiv 0, \quad (2)$$

subject to $M_i(0) = \bar{M}_i^o,\ i = 1, 2, \ldots.$ (3)

λ_i is the decay constant for nuclide *i*. The time point $t = 0$ is set at the time of waste package emplacement in the repository. All the packages of the same type are placed in the repository at the same time $t = 0$ and fail at the same failure time T_f. $\bar{M}_i^o$ is the mass of nuclide *i* in a single package at the time of package emplacement in the repository. The solution for $M_i(t)$ is readily available [4].

After the package failure, the balance equations are written as

$$\frac{dW_i(t)}{dt} = -\lambda_i W_i(t) + \lambda_{i-1} W_{i-1}(t) + NF_i(t),\ t > T_f,\ i = 1, 2, \ldots,\ \lambda_0 \equiv 0, \quad (4)$$

$$\text{subject to } W_i(T_f) = 0,\ \ i = 1, 2, \ldots, \quad (5)$$

$$\frac{dM_i(t)}{dt} = -\lambda_i M_i(t) + \lambda_{i-1} M_{i-1}(t) - F_i(t),\ t > T_f,\ i = 1, 2, \ldots,\ \lambda_0 \equiv 0, \quad (6)$$

subject to the value of $M_i(T_f)$ obtained by substituting $t = T_f$ in the solution to (2) as the initial condition.

In the last term of (4) and (6), the rate $F_i(t)$ of release from a failed waste package for radionuclide *i* is included. Note that from physical consideration $F_i(t) > 0$ if and only if $M_i(t) > 0$. Once $M_i(t)$ vanishes, so does $F_i(t)$.

Because the YMR consists of a single layer of a waste-package array with groundwater flowing downward perpendicular to the layer, and because the drift tunnels are separated with a sufficiently large distance of 81 m,[5] the release of radionuclides from a failed package

---

[4] M. Benedict, T. H. Pigford, and H. Levi, *Nuclear Chemical Engineering*, Chapter 8, 2nd ed., McGraw-Hill, 1981.

[5] Total System Performance Assessment - Analyses for Disposal of Commercial and DOE Waste Inventories at Yucca Mountain - Input to Final Environmental Impact Statement and Site Suitability Evaluation REV 00 ICN 02, 2001.

is not influenced by adjacent failed waste packages[6]. Therefore, in (4), $F_i(t)$ is multiplied by the total number N of waste packages of the same type in the repository[7].

Radionuclides are released by waste matrix dissolution either in congruent-release or solubility-limited mode[8].

For the congruent release, the release rate for nuclide *i* can be written as

$$F_i(t) = f_{\text{matrix}}(t) M_i(t), \qquad (7)$$

where $f_{\text{matrix}}(t)$ is the fractional dissolution rate of the matrix, defined as

$$f_{\text{matrix}}(t) \equiv \frac{F_{\text{matrix}}(t)}{M_{\text{matrix}}(t)}, \qquad (8)$$

with the dissolution rate $F_{\text{matrix}}(t)$ of the matrix and the mass $M_{\text{matrix}}(t)$ of the matrix remaining in a failed package.

For spent UN fuel, the matrix is considered to be UN including isotopes, ^{233}U, ^{234}U, ^{235}U, ^{236}U, and ^{238}U, while most DHLW is solidified by borosilicate glass. For UN, $M_{\text{matrix}}(t)$ and $F_{\text{matrix}}(t)$ are obtained by considering the mass and dissolution rate of UN in the package, respectively. For DHLW, these are for the mass and dissolution rate of silica. UN and borosilicate glass are assumed to dissolve in the solubility-limited release mode.

For the solubility-limited release, formulae for the rate of steady-state mass transfer by advection and diffusion from the surface of a cylindrical waste matrix were obtained in reference given in footnote 8. The dissolution rate $\dot{m}_i^*$ [mol/yr] of the dissolving species of nuclide *i* from the surface of the waste matrix was expressed as

$$\dot{m}_i^* = 8\varepsilon D_e C_i^* L \sqrt{Pe/\pi}, \text{ for } Pe > 4, \text{ where } Pe = \frac{U r_o}{D_e}. \qquad (9)$$

ε is the porosity of the surrounding porous rock. D_e [m^2/yr] is the diffusion coefficient of the dissolving chemical species of element *e*, in which isotope *i* is included. C_i^* [kg/m^3] is the solubility allocated for nuclide *i*. L [m] and r_o [m] are the length and the radius of the

---

[6] J. E. Houseworth, S. Finsterle, and G. S. Bodvarsson, Flow and Transport in the Drift Shadow in a Dual-Continuum Model, *J. Cont. Hydrology*, **62-63**, 133-156, 2003.

[7] J. Ahn, D. Kawasaki, P. L. Chambré, Relationship among Performance of Geologic Repositories, Canister-Array Configuration, and Radionuclide Mass in Waste, *Nuclear Technology*, **126**, 94-112, 2002.

[8] P. L. Chambré, T. H. Pigford, A. Fujita, T. Kanki, A. Kobayashi, H. Lung, D. Ting, Y. Sato, and S. J. Zavoshy, Analytical Performance Models for Geologic Repositories, LBL-14842, Lawrence Berkeley Laboratory, October 1982.

cylindrical waste package, U [m/yr] the ambient pore velocity of groundwater. Pe is the Peclet number, dimensionless.

The release rate for the solubility-limited release is written as

$$F_i(t) = \dot{m}_i^* . \qquad (10)$$

With $\dot{m}_i^*$, the fractional dissolution rate $f_i^*(t)$ for the solubility-limited release can be written as

$$f_i^*(t) = \dot{m}_i^*(t) \Big/ M_i(t). \qquad (11)$$

Whether the congruent release (7) or the solubility-limited release (10) is applied can be determined by comparing the fractional release rates $f_{\text{matrix}}(t)$ with $f_i^*(t)$. If $f_{\text{matrix}}(t) < f_i^*(t)$, then radionuclide i will be released congruently with the matrix dissolution. Otherwise, the nuclide will be released under the solubility-limited release mode. Thus, $F_i(t)$ is formulated for $t \geq T_f$ as follows:

$$F_i(t) = \begin{cases} \min\left(f_{\text{matrix}}(t) M_i(t), \dot{m}_i^* \right), \text{ while } M_{\text{matrix}}(t) > 0 \\ \dot{m}_i^*, \text{ for } M_{\text{matrix}}(t) = 0 \text{ and } M_i(t) > 0, \\ 0, \text{ for } M_i(t) = 0. \end{cases} \qquad (12)$$

where index i is for all nuclides except for those considered as the matrix.

For the solution for the problem given by (4), (5), (6) and (12), we consider an arbitrary time interval between t_o and $t_o + \Delta t$, for $t_o \geq T_f$. Within this time interval, we assume that the fractional dissolution rate $f_{\text{matrix}}(t)$ of the matrix is constant at the value $f_{\text{matrix}}(t_o)$. Then, the analytical solutions for the balance equations have been obtained, with which we have made numerical evaluations for $M_i(t)$ and $W_i(t)$ for $t \geq T_f$ in a stepwise manner.

IV.C. Data and Numerical Results

The dissolution rate of the UN was estimated to be approximately 7E-4 g/m^{2}h in de-aerated water at ambient temperature and > 9E-4 g/m^{2}h at 92^{o}C.[9] These values could be significantly reduced if a layer of UO_2 is formed on the surface of UN fuel pellets by exposure to water. Exposure to oxygen also results in the oxidation of a fresh surface of

[9] S. Sunder and N. H. Miller, *Corrosion of UN in Water*, AECL-11656, October 1996.

UN.[10] It is well known that UO_2 has low solubility in water.[11] Therefore, a UN sample covered with a UO_2 layer may appear unreactive in water. Such observations were also made in previous experiments.[12,]

Also from literature, for U metal, the dissolution rate was estimated to be ~28 g/m^2h in water at 100°C.[13] For U_3Si, it was between 9E-7 and 9E-5 g/m^2h at 100°C.[14] Thus, the dissolution rate for UN is much smaller than that for U metal but greater than that of U_3Si.

In YMR, where the host rock is partially saturated with water and in oxidative conditions, UN may have coatings of UO_2, resulting in significantly smaller dissolution rate of UN matrix.

Predicted rates of dissolution of the commercial-spent nuclear fuel (CSNF) were obtained as a function of temperature and pH for the TSPA calculations[15]; at 50°C and pH=7, the dissolution rate is shown to be 2E-4 g/m^2h.

With this value, 7,500 kg for the mass of uranium in a CSNF package and the geometrical surface area of the waste matrix is approximately 8 m^2, the time for completion of degradation has been calculated to be 3.8E5 years by the model described in the previous section.

For borosilicate glass in the DHLW, the dissolution rate is reported to be of the same order as the degradation rate of the CSNF fuel. The average mass of silica per Co-disposal package is approximately 7,700 kg, which is close to the mass of uranium in the CSNF package. Thus, the dissolution time for the DHLW has been calculated to be 3.9E5 years by the model.

From aforementioned comparisons, it may be reasonable to assume that the dissolution rate of UN would be greater than that of UO_2 in the YMR environment approximately by one order of magnitude. Assuming that the waste package for UN spent fuel has the same geometrical dimensions as those for the CNSF package, and contains the same mass of

---

[10] K. Ikawa and K. Taketani, Room Temperature Oxidation of Uranium Nitride Powder, *Journal of Nuclear Science and Technology*, **7(9)**, 433-438, 1970.
[11] D. W. Shoesmith, S. Sunder, and W. H. Hocking, Electrochemistry of UO_2 Nuclear Fuel, VCH Publishers Inc., New York, NY, 297-337, 1994.
[12] S. Sugihara and S. Imoto, Hydrolysis of uranium nitrides, *Journal of Nuclear Science and Technology,* **6**, 237-242, 1969.
[13] W. T. Bourns, *Corrosion testing of uranium silicide fuel specimens,* AECL-2718, 1968.
[14] W. T. Bourns, A literature survey of U_3Si corrosion, AECL-2609, 1967.
[15] Yucca Mountain Science and Engineering Report, US Department of Energy, Office of Civilian Radioactive Waste Management, DOE/RW-0539-1, February 2002. http://www.ocrwm.doe.gov/documents/feis_2/index.htm

uranium, the dissolution time for UN spent fuel package has been calculated to be 3.5E4 years, which is about a factor of 10 smaller than those for CSNF and DHLW.

In this analysis, detailed calculations for radionuclide release and accumulation in the environment have not been made. With results of burn-up calculations for UN fuel, quantitative evaluations for cumulative radionuclide release can be made. If the dissolution time of the UN spent fuel is of the order of a few tens of thousands of years, mass of Pu-239 in the spent fuel would affect the environmental impact from the UN spent fuel disposal significantly.

IV.D. Summary

The estimate shown in this chapter is subject to many uncertainties and assumptions, and is semi-quantitative. The reported high dissolution rates of UN in water at ~ 92°C indicate that UN is not stable in the hot aqueous environment. The numerical evaluation, based on the assumption that the dissolution rate of UN spent fuel is 10 times greater than those for UO_2 and borosilicate glass, indicates that the dissolution of UN spent fuel would complete within the time duration comparable to the half-life of Pu-239.